Journal of Power Sources 185 (2008) 1359–1366

Contents lists available at ScienceDirect

Journal of Power Sources

journal homepage: www.elsevier.com/locate/jpowsour

Surface reactions and performance of non-aqueous electrolytes with lithium metal anodes

Li Yang[a], Carl Smith[a], Charles Patrissi[b], Christian R. Schumacher[b], Brett L. Lucht[a,*]

[a] University of Rhode Island, Department of Chemistry, 51 Lower College Rd., Kingston, RI 02881, United States
[b] Naval Undersea Warfare Center, Newport, RI 02841, United States

ARTICLE INFO

Article history:
Received 24 July 2008
Received in revised form
10 September 2008
Accepted 11 September 2008
Available online 20 September 2008

Keywords:
Lithium battery
Electrolytes
Electrode passivation

ABSTRACT

Six electrolytes were investigated for lithium metal battery applications. The electrolytes were composed of combinations of four different salts ($LiPF_6$, $LiB(C_2O_4)_2$, LiI and $LiN(SO_2CF_3)_2$) and three different solvents (PC, DME, and 1,3-dioxolane). All six electrolytes had conductivities >3 mS cm^{-1} at temperatures from −20 to 40 °C. Electrochemical impedance spectroscopy (EIS) and linear polarization, both at room temperature and low temperature (−8 °C), provided congruent results. The LiI-based electrolyte had the lowest film resistance, while 0.7 M $LiB(C_2O_4)_2$–PC:DME (1:1) had the highest impedance. The presence of 1,3-dioxolane in electrolytes provided lower impedance with $LiB(C_2O_4)_2$ but higher resistance with $LiPF_6$-based electrolytes. NMR analysis of electrolytes after thermal abuse indicate that $LiN(SO_2CF_3)_2$-based electrolytes are the most thermally stable. SEM analysis suggests that surface modification and impedance changes are correlated.

© 2008 Elsevier B.V. All rights reserved.

1. Introduction

While lithium metal secondary batteries received significant interest in the early 1990s, problems primarily associated with the generation of lithium dendrites upon cycling shifted research away from lithium metal anodes [1]. However, the development of lithium metal primary batteries continued [2]. In an effort to develop lithium metal primary batteries with good performance characteristics at low temperature (−8 °C) and long shelf lives (>1 year), we have conducted a detailed investigation of the thermal stability, surface reactions, and interfacial resistance of six different electrolytes. The electrolytes contain four different salts, $LiPF_6$, $LiB(C_2O_4)_2$ (LiBOB), $LiN(SO_2CF_3)_2$ (LiTfSI), and LiI, dissolved in combinations of up to three different solvents, propylene carbonate (PC), dimethoxyethane (DME), and 1,3-dioxalane. The salts and solvents were selected after a review of the lithium-ion secondary and lithium metal primary battery electrolyte literature [2–4].

It is well known that a solid–electrolyte interphase (SEI) is spontaneously formed via reaction of lithium metal with most non-aqueous electrolytes [1]. The SEI is primarily composed of the decomposition products of the salts and solvents and provides a passivation layer inhibiting further electrolyte reduction [5]. Formation of a stable SEI is critical to the performance of lithium metal batteries. Understanding the role of the salt and solvent in the composition of SEI is very important to develop lithium metal batteries with a wide temperature range and good shelf life.

2. Experimental

Lithium hexafluorophosphate ($LiPF_6$) was obtained from Hashimoto Chemical Corporation. Lithium bisoxalatoborate (LiBOB) was provided by Chemetal, Germany. Lithium iodide (LiI) (99.99%) and lithium bis(trifluoromethanesulfonyl)imide (LiTfSI) (99.95%) were purchased from Aldrich. The LiBOB, LiI and LiTfSI were vacuum dried at 80 °C for 24 h. PC (battery grade, H_2O <20 ppm) was obtained from EM Industries. Anhydrous DME (H_2O <30 ppm) and 1,3-dioxolane (H_2O <50 ppm) were purchased from Aldrich. All solvents were stored over 3 Å molecular sieves for 2 weeks before use. Dimethyl acetamide (DMAc) and tributylamine (TBA) were purchased anhydrous from Aldrich without further treatment. The electrolytes were prepared in an Ar-filled glove box with H_2O <0.1 ppm. Electrolyte compositions are given in Table 1, wherein all ratios are volume ratios except the additives, whose ratios are weight ratios. Concentration of $LiPF_6$-based electrolytes is set to be 1.0 M, a typical concentration used in the lithium-ion battery industry. LiBOB-based concentration is set to be 0.7 M, due to its poor solubility [3]. The concentration of LiI-based electrolyte is referred to literature [2]. LiTfSI-based electrolytes is set to be 0.75 M, since the large anion volume compared to the other three

* Corresponding author. Tel.: +1 401 874 5071; fax: +1 401 874 5072.
E-mail address: blucht@chm.uri.edu (B.L. Lucht).

0378-7753/$ – see front matter © 2008 Elsevier B.V. All rights reserved.
doi:10.1016/j.jpowsour.2008.09.037

Table 1
Electrolyte compositions and abbreviations used in this report.

1	$LiPF_6$-1	1.0 M $LiPF_6$–PC/DME (1:1), plus 1000 ppm DMAc
2	$LiPF_6$-2	1.0 M $LiPF_6$–PC/DME/1,3-dioxolane (1:1:1), plus 3000 ppm TBA
3	LiBOB-1	0.7 M LiBOB–PC:DME (1:1)
4	LiBOB-2	0.7 M LiBOB–PC:DME:1,3-dioxolane (1:1:1)
5	LiI	0.75 M LiI–DME:1,3-dioxolane (1:2)
6	LiTfSI	0.75 M LiTfSI–DME:1,3-dioxolane (1:2)

salts which introduces a high viscosity into the electrolyte as concentration increases [3].

The conductivities of the electrolytes were measured with a 712 Conductometer from Metrohm Ltd. at several temperatures: −20, 0, 20, and 40 °C. The physical properties of the solvents are listed in Table 2. Two lithium/electrolyte/lithium coin cells (NRC-ICPET, 23 mm in diameter) for each electrolyte were prepared. The surface area of the counter/reference lithium foil is 2.3 cm^2, while the working lithium foil has a surface area of 0.8 cm^2. Cell to cell variation was less than 5%. Electrochemical impedance spectroscopy (EIS) and linear (dc) polarization analysis of the coin cells were performed using a 263A potentiostat/galvanostat (Princeton Applied Research). The EIS frequency ranged from 100 kHz to 0.1 Hz in order to study the evolution of the SEI without the risk of charge–discharge behavior damaging the SEI film at lower frequencies. The EIS ac perturbation amplitude was 2.5 mV for room temperature measurements and 5.0 mV for low temperature (−8 °C) measurements. Linear polarization analysis was performed by cyclic voltammetry (CV) at a scanning rate of 0.02 mV s^{-1} from the open circuit voltage – 0.0 mV in the case of Li/Ele/Li – to 10.0 mV. The contribution of cell resistances to polarization was determined as the slopes of the linear plots.

Samples for NMR spectroscopy were prepared in an Ar-filled glove box. NMR sample tubes were flame-sealed and stored for set amounts of time at 80 °C. NMR spectroscopy was performed using a JEOL 400 MHz NMR spectrometer. ^{13}C NMR, ^{19}F NMR and ^{11}B NMR spectra were collected using a single pulse method. Spectra references were ^{13}C TMS at 0 ppm, ^{19}F $LiPF_6$ at 65.0 ppm and ^{11}B LiBOB at 6.5 ppm. GC–MS analyses were obtained on an Agilent Technologies 6890 GC with a 5973 Mass Selective Detector and a HP-5MS Column. Helium was used as the carrier gas with a flow rate of 3.3 mL min^{-1}. Samples were ramped from 30 to 250 °C at 10 °C min^{-1}. Scanning electron microscopy (SEM) analyses of the soaked lithium metal electrodes were conducted on a JEOL-5900 Scanning Electron Microscope. Samples were rinsed by anhydrous DME and dried under vacuum overnight and transferred from glove box to SEM chamber in a sealed transport container filled with argon.

3. Results and discussion

3.1. Conductivity of the electrolytes

The temperature dependence of $LiPF_6$- and LiBOB-based electrolytes have similar trends. There is a steady decrease in conductivity with decreasing temperature (Fig. 1). The incorporation of the lower viscosity solvent, 1,3-dioxolane, increases the conductivity by 3–4 mS cm^{-1} for $LiPF_6$-based electrolytes and by ~1 mS cm^{-1} for LiBOB-based electrolytes.

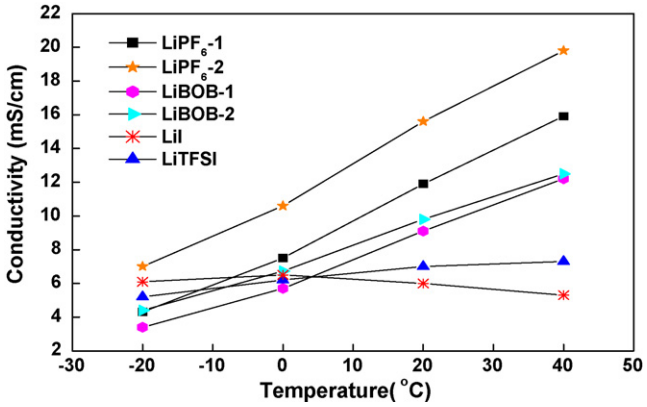

Fig. 1. Conductivity of prepared electrolytes vs. temperature.

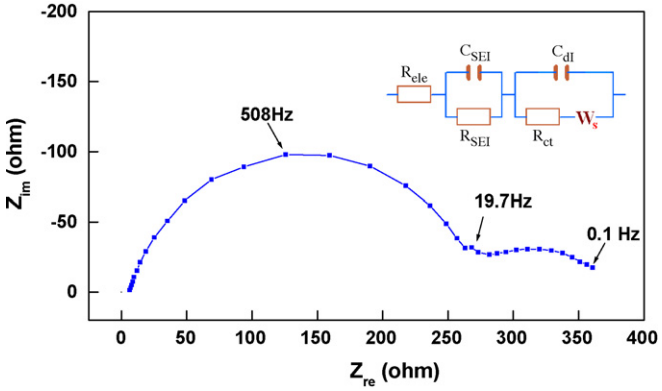

Fig. 2. Typical EIS Nyquist plot for Li/Ele/Li cell.

The conductivity of the LiI-based electrolyte is largely temperature independent with a slight trend toward increasing conductivity with decreased temperature [2]. Similar trends have been reported with alkali metal salts in ethereal solvents with low dielectric constants [6]. LiTfSI has a slight decrease in conductivity when temperature decreases. The high dissociation constant and large size of the LiTfSI anion makes it suitable for solvents with lower dielectric constants [3] which result in low viscosity.

3.2. EIS impedance

A typical Li/Ele/Li cell impedance spectrum and equivalent circuit are provided in Fig. 2. The semicircle in the high to intermediate frequency range is attributed primarily to the SEI impedance, along with some charge transfer resistance which is typically small in comparison [7–9]. From 19.7 to 0.1 Hz, there is a curve approaching $Z_{im} = 0$. This has been associated with finite length diffusion phenomena on a non-blocking electrode [10,11].

Impedance spectra for the anode SEI measured at 25 °C over time are provided in Fig. 3. The initial impedances, R_{SEI}, range from about 125 Ω for LiI to 325 Ω for LiBOB-1. Upon storage of the cells at room temperature for 15 days a small impedance rise was observed

Table 2
Physical properties of solvents [4].

	Acronym	Dielectric constant	Viscosity (cP)	Melting point (°C)
Propylene carbonate	PC	64.95	2.51	−48.8
1,2-Dimethoxy ethane	DME	7.075	0.407	−58
1,3-Dioxolane		7.13	0.589	−95

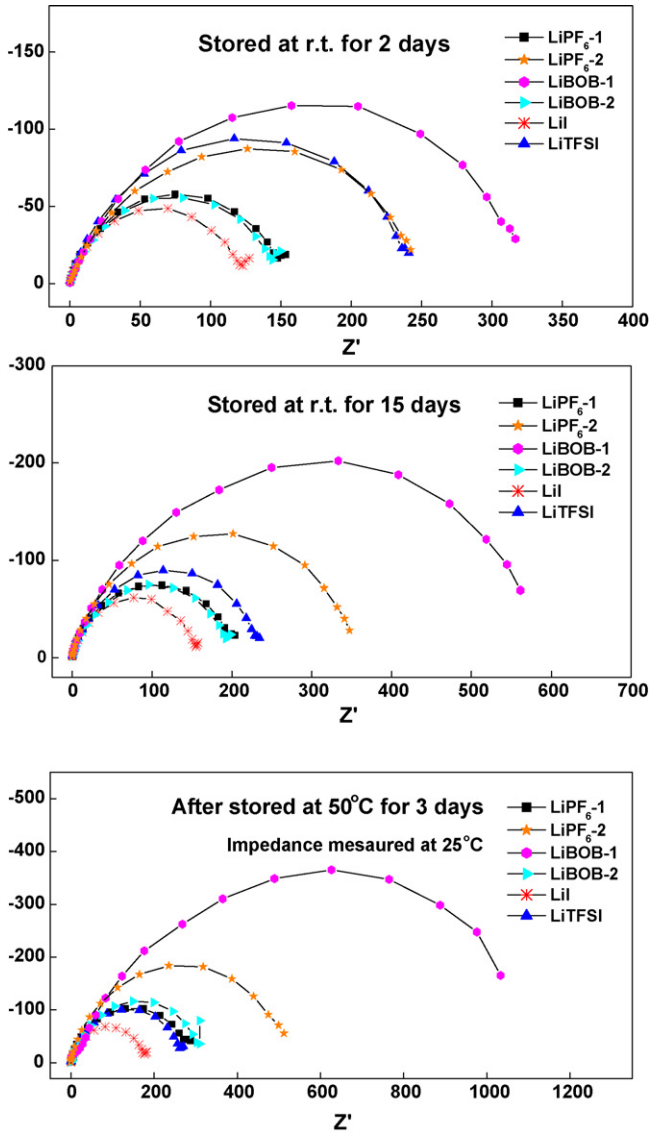

Fig. 3. SEI impedance vs. time, all measured at 25 °C.

for all electrolytes except LiTfSI. After storage at room temperature for 15 days the cells were exposed to elevated temperature (50 °C) for 3 days to simulate accelerated aging. After the accelerated aging the cell containing LiI-based electrolyte had the lowest impedance. Both the LiI and LiTFSI electrolytes had only small increases (15% and 13%, respectively) in the impedance after storage at elevated temperature.

A significant increase in impedance was observed for all of the other electrolytes. The increase was greatest for LiBOB-1 (85%) followed by $LiPF_6$-2 (48%), LiBOB-2 (60%) and $LiPF_6$-1 (45%). The impedance increases suggest that there is a complex relationship between the electrolyte composition (salt and solvent) and the development of the SEI layer. The incorporation of 1,3-dioxolane decreases the impedance for LiBOB-based electrolytes, LiBOB-1 vs. LiBOB-2, but increases the impedance of $LiPF_6$-based electrolytes, $LiPF_6$-2 vs. $LiPF_6$-1. This suggests that both the salt and the solvent are involved in surface film formation on lithium metal electrodes. In the case of LiBOB electrolytes, the reaction of the 1,3-dioxolane on the surface of Li may prevent further decomposition reactions of the LiBOB salt. However, the Lewis acidity of $LiPF_6$ (via generation of PF_5) may catalyze polymerization of 1,3-dioxolane thus increasing the impedance [12].

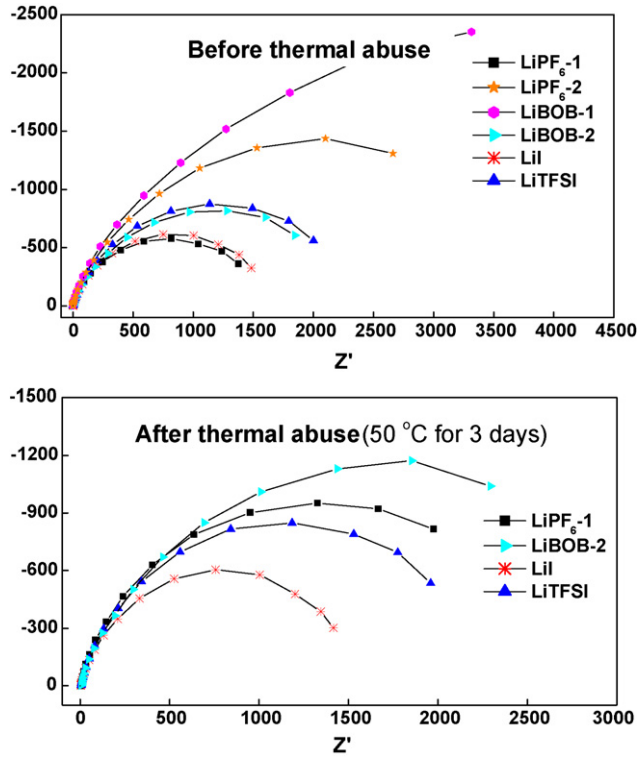

Fig. 4. EIS spectra measure at −8 °C, before and after storage at 50 °C for 3 days.

Fig. 4 contains impedance measured at −8 °C, before and after high temperature storage (50 °C for 3 days). The impedance spectra for $LiPF_6$-2 and LiBOB-1 after accelerated aging are not provided due to the extremely high resistances. The impedance trend at −8 °C is similar to that observed at 25 °C. The impedance of each cell at −8 °C is roughly 10 times the impedance of the same cell at 25 °C. The SEI film impedances are summarized in Fig. 5.

3.3. Linear (dc) polarization

In addition to EIS, linear (dc) polarization analysis provides further information about SEI film resistance [13–15]. Representative data is provided in Fig. 6. The slope of the linear fit of the data provides the cell resistance. The polarization resistances of thermal abused cells determined by dc polarization are shown in Fig. 7 and generally agree with those determined by EIS. The low-temperature resistance is about 10 times of the resistance at 25 °C. The cells show the following trend in resistance: LiI ≈ LiTfSI < $LiPF_6$-1 ≈ LiBOB-2 < $LiPF_6$-2 < LiBOB-1.

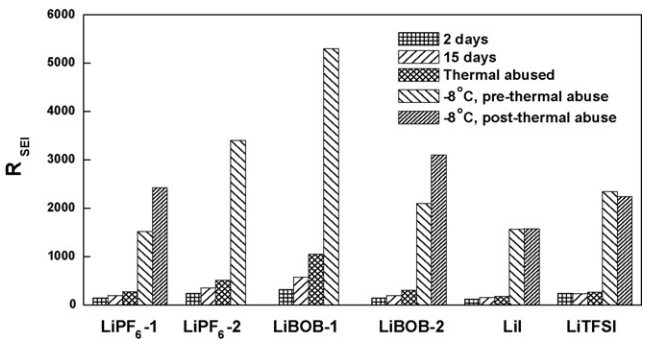

Fig. 5. Summary of SEI impedance.

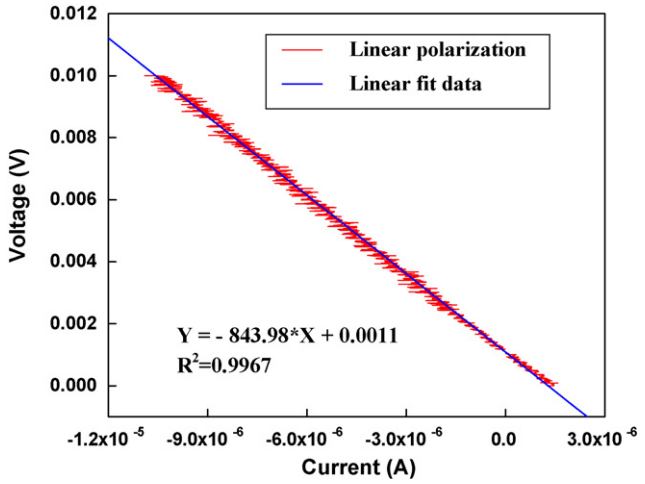

Fig. 6. Typical linear polarization data.

3.4. Thermal stability of the electrolytes

3.4.1. $LiPF_6$-based electrolyte

The thermal instability of $LiPF_6$ in carbonate and ethereal solvents is well known [16–18]. Storage of $LiPF_6$ at elevated temperature (>75 °C) results in the thermal dissociation of $LiPF_6$ to LiF and PF_5. The Lewis acidity of PF_5 is largely responsible for the reaction with solvent [16]. While the reactions of $LiPF_6$ or PF_5 with carbonates and simple ethers have been previously reported [18], interest in utilizing DME and 1,3-dioxolane in lithium battery electrolytes prompted further investigation. Storage of 0.5 M $LiPF_6$ in DME at 80 °C for 3 days results in discoloration of the electrolyte and the appearance of new resonances by ^{13}C and ^{19}F NMR spectroscopy (Figs. 8 and 9). The new ^{19}F resonances are consistent with the generation of fluorophosphates (OPF_2OR and $OPF(OR)_2$). The new ^{13}C resonances are consistent with formation of diglyme and dimethyl ether. The thermally abused electrolyte was analyzed by GC–MS and structurally assigned through matching to the National Institutes of Standards (NIST) library (Fig. 10). Phosphorus oxyfluoride along with dimethyl ether and diglyme are observed as expected from solvent disproportionation reactions. Upon incorporation of 1 wt.% DMAc to 0.5 M $LiPF_6$ in DME the thermal decomposition is dramatically inhibited. Electrolytes with DMAc can be stored at 80 °C for 3 days with little evidence for decomposition [19].

The thermal stability of 1,3-dioxolane in $LiPF_6$ is significantly lower than DME. Preparation of a 0.5 M $LiPF_6$ solution of 1,3-dioxolane results in the generation of poly-dioxolane upon storage at room temperature for 3 h, as evidenced by ^{13}C NMR spectroscopy (Fig. 11). Unfortunately, addition of the moderate Lewis basic additive DMAc does not suppress the polymerization of 1,3-dioxolane. However, addition of the strong Lewis base tributylamine (TBA, 1 wt%) significantly reduced the polymerization reaction [20]. The

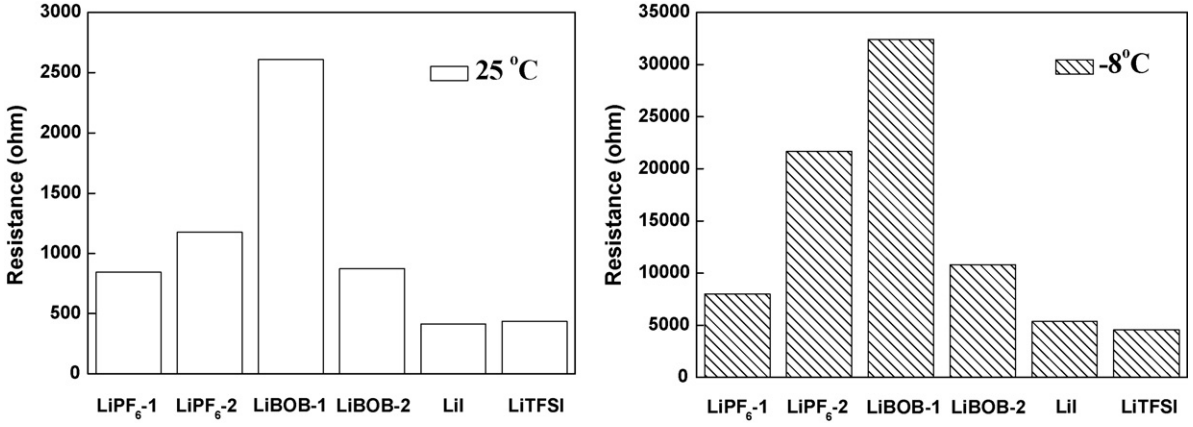

Fig. 7. Polarization resistance of thermal abused coin cells at 25 and −8 °C, respectively.

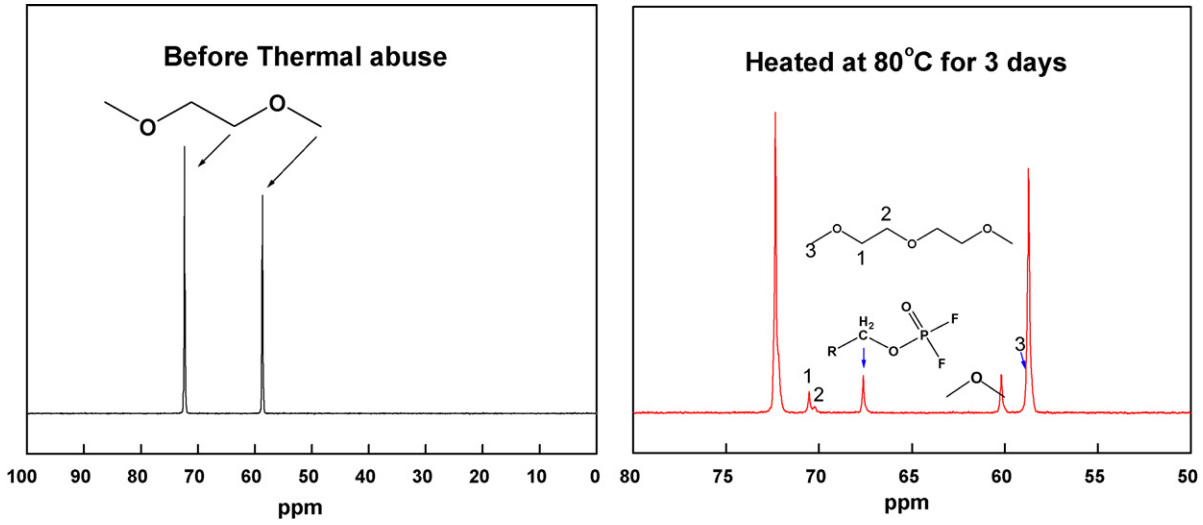

Fig. 8. ^{13}C NMR of 0.5 M $LiPF_6$ in DME without additives.

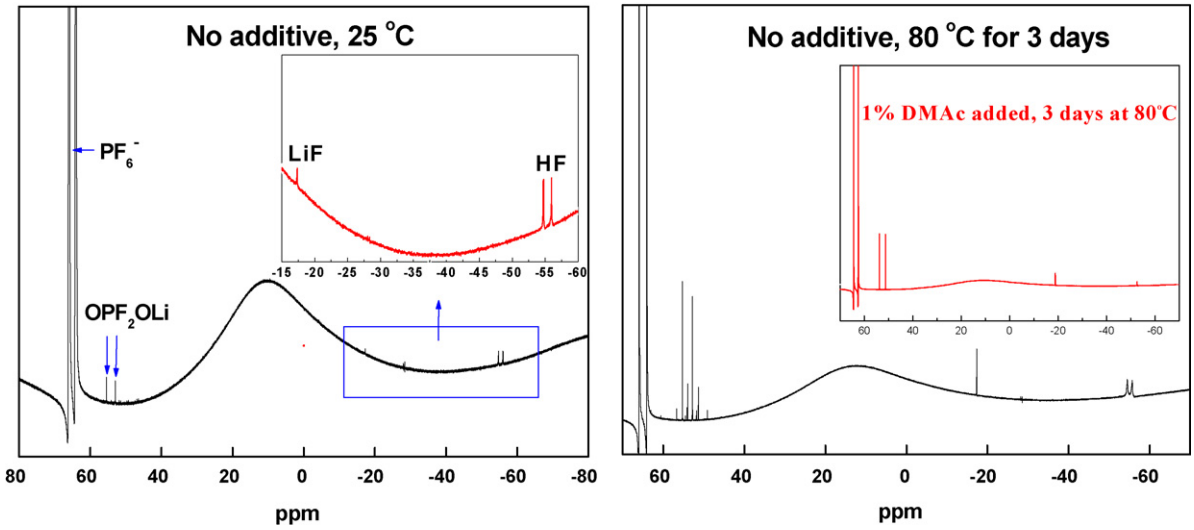

Fig. 9. ^{19}F NMR of 0.5 M $LiPF_6$ in DME.

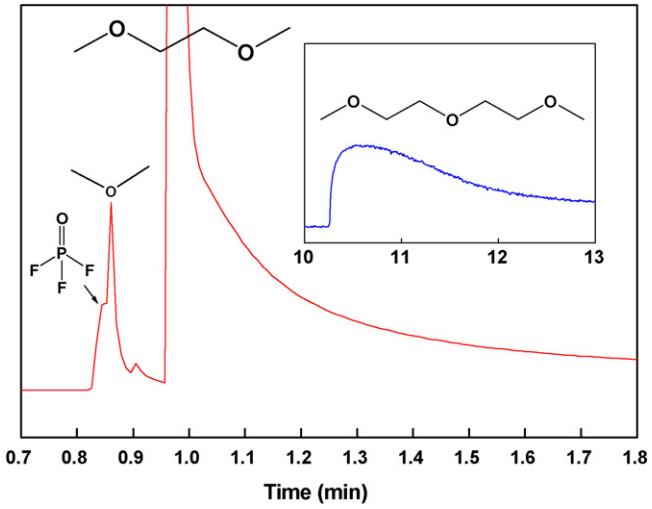

Fig. 10. GC traces of 0.5 M $LiPF_6$ in DME.

instability of $LiPF_6$/1,3-dioxolane-based electrolytes is shown by the higher impedances observed for $LiPF_6$ electrolytes containing 1,3-dioxolane.

3.4.2. *LiBOB-based electrolytes*

Storage of LiBOB in PC at 80 °C for 5 days provides no evidence for decomposition of either PC or LiBOB. This supports previous investigations suggesting that LiBOB/carbonate electrolytes are thermally stable [21]. A single resonance for LiBOB is observed at 6.5 ppm in ^{11}B NMR spectra. Storage of the 0.7 M LiBOB–PC:DME (1:1)-based electrolyte at 80 °C for 5 days results in precipitation and decomposition of LiBOB. A new ^{11}B resonance at 4.2 ppm consistent with the formation of a new tetravalent boron species is observed [22].

Storage of the 0.7 M LiBOB–PC:DME:1,3-dioxolane (1:1:1) electrolyte at 80 °C for 5 days resulted in decomposition of both LiBOB and the solvent. Peaks characteristic of poly-dioxolane and other ethereal side products are observed by ^{13}C NMR spectroscopy. Two new broad resonances (8.3 and 22.0 ppm) are observed in ^{11}B NMR spectra (Fig. 12), consistent with the formation of trivalent and tetravalent borane species, respectively [22–25]. Related species are observed upon reaction of LiBOB with methanol. LiBOB is quantitatively converted to $B(OMe)_3$ (17.7 ppm, ^{11}B) and $LiB(OMe)_4$

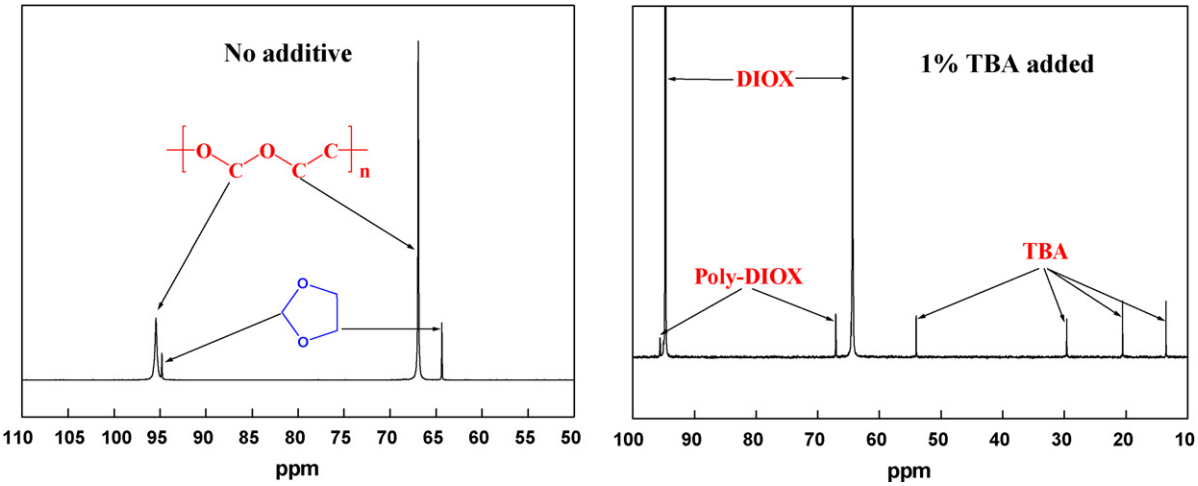

Fig. 11. ^{13}C NMR of 0.5 M $LiPF_6$ in 1,3-dioxolane (25 °C, without heating).

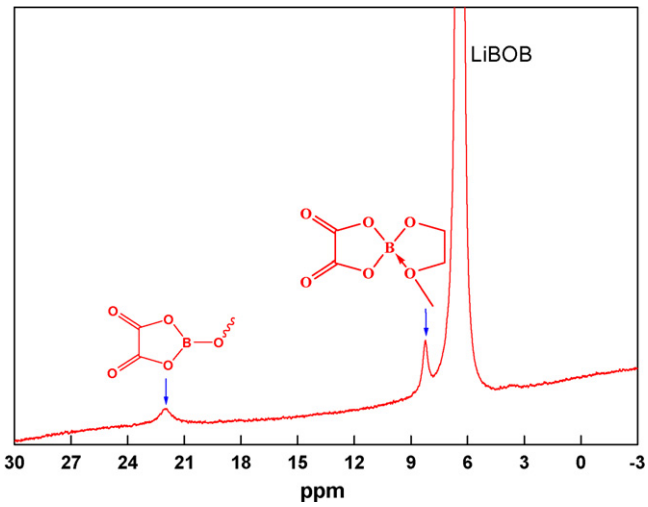

Fig. 12. ^{11}B spectra of 0.7 M LiBOB–PC:DME:1,3-dioxolane (1:1:1), stored at 80 °C for 5 days.

(4.3 ppm, ^{11}B) upon storage in methanol at room temperature for 24 h.

3.4.3. LiI-based electrolytes

There is little spectroscopic evidence for the decomposition of LiI in DME and 1,3-dioxolane. However, there is a slight yellowing of the solution over time which probably results from the generation of low concentrations of I_2 in solution.

3.4.4. LiTfSI-based electrolytes

LiTfSI-based electrolytes are stable to thermal abuse by the NMR analysis. There is no evidence for either solvent or salt decomposition upon storage at 80 °C for 5 days. The outstanding thermal stability of solid LiTfSI has been previously reported [26].

3.5. SEM of the electrodes

Changes to the surface of lithium metal upon exposure to the different electrolytes were analyzed by SEM. The lithium metal was soaked in electrolyte for 2 weeks at room temperature followed by SEM analysis. The pristine lithium metal has light uniform parallel striations (Fig. 13). In addition, there are some faint irregular features on the surface.

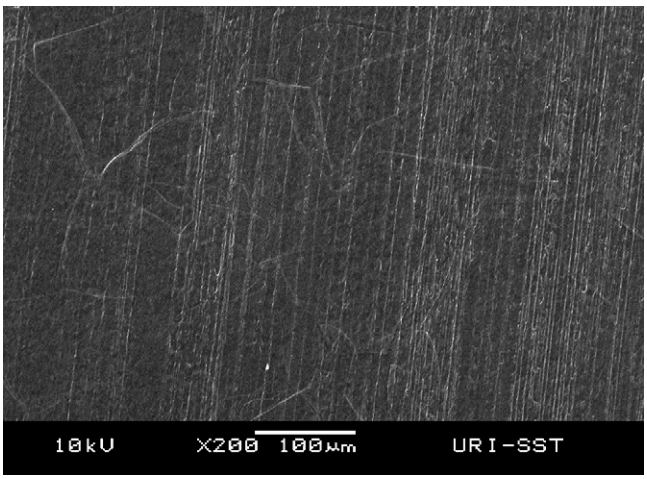

Fig. 13. SEM image of pristine lithium.

Storage of lithium metal in the presence of $LiPF_6$ electrolytes results in significant changes to the surface of the metal (Fig. 14). The striations are significantly deeper and less uniform while the irregular features are more pronounced. The changes to the surface are consistent with either an etching of the surface by the electrolyte or deposition of electrolyte decomposition products on the surface of the lithium metal. The surface modification correlates with the observed increase in impedance. However, the differences between $LiPF_6$ electrolytes with and without 1,3-dioxolane are small.

Changes to the surface of lithium metal are also observed upon storage in the presence of LiBOB-based electrolytes (Fig. 15). Samples containing LiBOB have only small changes in both the light uniform striations and faint irregular features, but there is a generation of new granular particles on the surface. The appearance of the new particles suggests that the reactions of the LiBOB electrolytes are either initiated by surface defects or that the initial electrolyte decomposition products initiate localized degradation of the electrolyte. Regardless, LiBOB electrolytes significantly modify the metal surface.

Samples of lithium soaked in 0.75 M LiI–DME:1,3-dioxolane (1:2) provide similar results to the $LiPF_6$ electrolytes (Fig. 16). The depth of the striations is increased with little change in the irregular features. The surface of the lithium metal exposed to LiTfSI electrolyte is very similar to the pristine lithium suggesting only

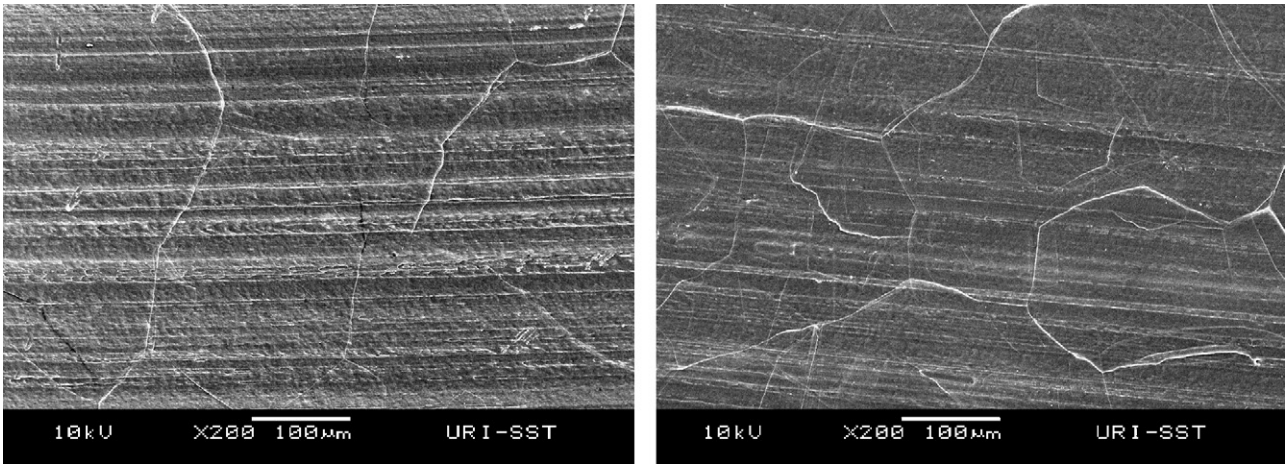

Fig. 14. SEM images of lithium–1.0 M $LiPF_6$–PC/DME (1:1) (left) and 1.0 M $LiPF_6$–PC/DME/1,3-dioxolane (1:1:1) (right).

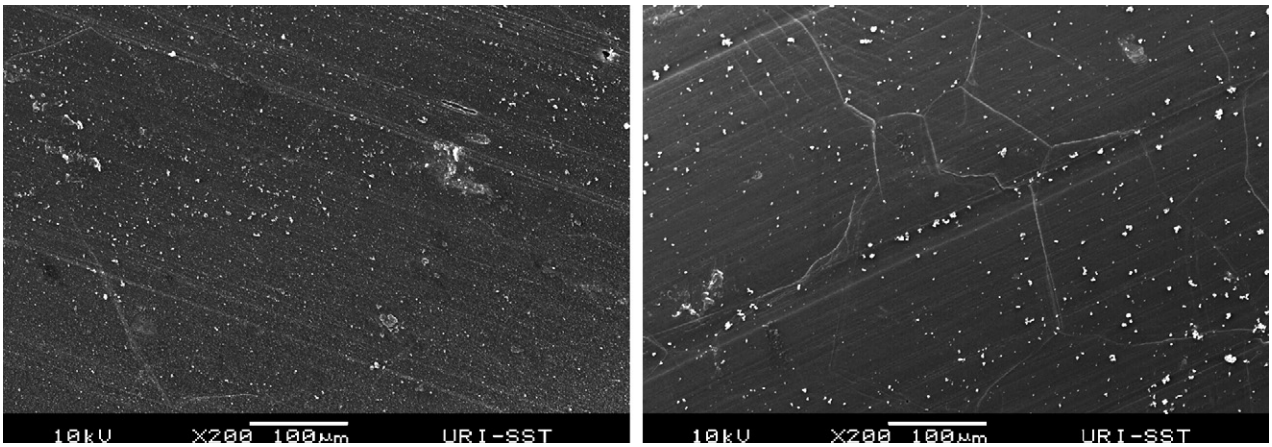

Fig. 15. SEM images of lithium–0.7 M LiBOB–PC:DME (1:1) (left) and 0.7 M LiBOB–PC:DME:1,3-dioxolane (1:1:1) (right).

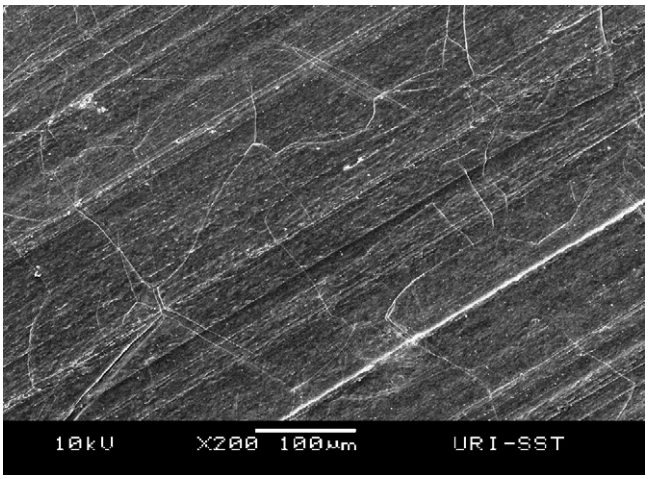

Fig. 16. SEM images of lithium–0.75 M LiI–DME:1,3-dioxolane (1:2).

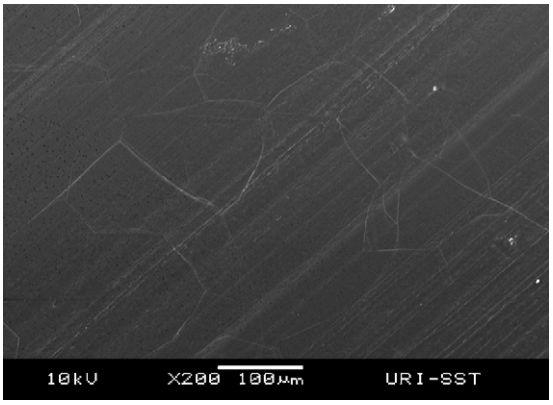

Fig. 17. SEM image of lithium–0.75 M LiTfSI–DME:1,3-dioxolane (1:2).

small changes to the surface, consistent with the impedance data (Fig. 17).

4. Conclusion

Six electrolytes based on different lithium salts and solvents were investigated by conductivity, EIS, linear polarization, NMR spectroscopy, and SEM. Conductivities of the $LiPF_6$- and LiBOB-based electrolytes depend strongly on temperature, whereas the LiTfSI- and LiI-based electrolytes have little temperature dependence between −20 and +40 °C. EIS and linear polarization indicate that the LiI-based electrolyte has the smallest surface film resistance both at room temperature and at −8 °C, while 0.7 M LiBOB–PC:DME (1:1) has highest resistance of all electrolytes. The addition of 1,3-dioxolane greatly reduces the resistance of LiBOB-based electrolytes but increases the resistance of $LiPF_6$ electrolytes. The thermal stability of the electrolytes was investigated by NMR spectroscopy. LiI and LiTfSI electrolytes have very good stability while the stability of LiBOB and $LiPF_6$ is lower, especially in the presence of 1,3-dioxolane. SEM surface analysis generally supported the EIS and linear polarization data, suggesting the modification of the lithium metal surface is largely responsible for the changes in resistance.

Acknowledgements

We thank the Partnership for Ocean Instrumentation (POI) at the University of Rhode Island and the Naval Undersea Warfare Center, Division Newport for partial support of this research. Yardney Technical Products (Lithion) for assistance with conductivity measurements. The sensor and Surface Technology Partnership at URI for assistance with SEM. Chemetal for generous donation of LiBOB.

References

[1] M. Wakihara, O. Yamamoto (Eds.), Lithium Ion Batteries: Fundamentals and Performance, Wiley–VCH, New York, 1998.
[2] A. Weber, D.A. Kaplin, Proceedings of the 41st Power Sources Conference, June 14–17, 2004, pp. 53–56.
[3] K. Xu, Chem. Rev. 104 (2004) 4303.
[4] D. Aurbach (Ed.), Nonaqueous Electrochemistry, Marcel Dekker, New York, 1999.
[5] P.B. Balbuena, Y. Wang (Eds.), Lithium-Ion Batteries: Solid–Electrolyte Interphase, Impereal College Press, London, 2004.
[6] M.C. Day, H.M. Barnes, A.J. Cox, J. Phys. Chem. 68 (1964) 2595.
[7] M.W. Verbagree, B.I. Koch, J. Electroanal. Chem. 367 (1994) 123.
[8] D. Aurbach, A. Zaban, J. Electrochem. Soc. 348 (1993) 155–179.
[9] E. Peled, H. Yamin, J. Power Sources 9 (3–4) (1983) 253–266.
[10] V. Gentili, S. Panero, P. Reale, B. Scrosati, J. Power Sources 170 (2007) 185–190.
[11] S.S. Zhang, et al., J. Power Sources 154 (2006) 276–280.
[12] O. Youngman, P. Dan, D. Aurbach, Electrochim. Acta 35 (1990) 639.
[13] M.C. Smart, R.V. Bugga, S. Surampudi, C. Huang, US Patent 6,492,064.
[14] M.C. Smart, B.L. Lucht, B.V. Ratnakumar, J. Electrochem. Soc. 155 (2008) A557.
[15] N. Munichandraiah, L.G. Scanlon, R.A. Marsh, B. Kumar, A.K. Sircar, J. Electroanal. Chem. 179 (1994) 495.
[16] C.L. Campion, W. Li, B.L. Lucht, J. Electrochem. Soc. 152 (2005) A2327–A2334.
[17] S.E. Sloop, J.K. Pugh, S. Wang, J.B. Kerr, K. Kinoshita, Electrochem. Solid-State Lett. 4 (2001) A42.
[18] R.A. Goodrich, P.M. Treichel, J. Am. Chem. Soc. 88 (1966) 3509.

[19] W. Li, B.L. Lucht, Electrochem. Solid-State Lett. 10 (2007) A115.
[20] D. Aurbach, I. Weissman, A. Zaban, Y. Ein-Eli, E. Mengeritsky, P. Dan, J. Electrochem. Soc. 143 (1996) 2110.
[21] A. Xiao, L. Yang, B.L. Lucht, Electrochem. Solid-State Lett. 10 (2007) A241.
[22] P. Laszlo (Ed.), NMR of Newly Accessible Nuclei, Chemically and Biochemically Important Elements, vol. 2, Academic Press, New York, 1983, p. 56.
[23] K. Xu, U. Lee, S.S. Zhang, M. Wood, R.T. Jow, Electrochem. Solid-State Lett. 6 (2003) A144.
[24] K. Xu, U. Lee, S.S. Zhang, T.R. Jow, J. Electroanal. Chem. 151 (2004) A2106.
[25] E.F. Mooney, M.G. Anderson (Eds.), Annual Review of NMR Spectroscopy, vol. 2, Academic Press, New York, 1969, p. 219.
[26] H. Nöth, H. Vahrenkamp, Chem. Ber. 99 (1966) 1049.